

See discussions, stats, and author profiles for this publication at:  
<https://www.researchgate.net/publication/223832161>

# Chemical mechanism and substrate binding sites of NADP-dependent aldehyde dehydrogenase from *Streptococcus mutans*

ARTICLE *in* CHEMICO-BIOLOGICAL INTERACTIONS · FEBRUARY 2001

Impact Factor: 2.58 · DOI: 10.1016/S0009-2797(00)00218-0

---

CITATIONS

24

---

READS

22

6 AUTHORS, INCLUDING:



Frédérique Favier

University of Lorraine

29 PUBLICATIONS 919 CITATIONS

SEE PROFILE



Guy Branlant

University of Lorraine

152 PUBLICATIONS 3,443 CITATIONS

SEE PROFILE



ELSEVIER

## Chemical mechanism and substrate binding sites of NADP-dependent aldehyde dehydrogenase from *Streptococcus mutans*

Stéphane Marchal <sup>a</sup>, David Cobessi <sup>b</sup>,  
Sophie Rahuel-Clermont <sup>a</sup>, Frédérique Tête-Favier <sup>b</sup>,  
André Aubry <sup>b</sup>, Guy Branlant <sup>a,\*</sup>

<sup>a</sup> Laboratoire de Maturation des ARN et Enzymologie Moléculaire, UMR 7567 CNRS-UHP,  
Faculté des Sciences, BP 239, 54506 Vandoeuvre-lès-Nancy, France

<sup>b</sup> Laboratoire de Cristallographie et Modélisation des Matériaux Minéraux et Biologiques,  
Groupe Biocristallographie, ESA 7036, Faculté des Sciences, BP 239,  
54506 Vandoeuvre-lès-Nancy, France

### Abstract

Non-phosphorylating glyceraldehyde 3-phosphate dehydrogenase from *Streptococcus mutans* (GAPN) belongs to the aldehyde dehydrogenase (ALDH) family, which catalyzes the irreversible oxidation of a wide variety of aldehydes into acidic compounds via a two-step mechanism: first, the acylation step involves the formation of a covalent ternary complex ALDH-cofactor-substrate, followed by the oxidoreduction process which yields a thioacyl intermediate and reduced cofactor and second, the rate-limiting deacylation step. Structural and molecular factors involved in the chemical mechanism of GAPN have recently been examined. Specifically, evidence was put forward for the chemical activation of catalytic Cys-302 upon cofactor binding to the enzyme, through a local conformational rearrangement involving the cofactor and Glu-268. In addition, the invariant residue Glu-268 was shown to play an essential role in the activation of the water molecule in the deacylation step. For E268A/Q mutant GAPNs, nucleophilic compounds like hydrazine and hydroxylamine were shown to bind and act as substrates in this step. Further studies were focused at understand

**Abbreviations:** GAPN, non-phosphorylating glyceraldehyde 3-phosphate dehydrogenase; G3P, glyceraldehyde 3-phosphate;  $k_{ac}$ , acylation rate constant;  $k_{ss}$ , steady state rate constant; SIE, solvent isotope effect;  $k_2$ , second order rate constant.

\* Corresponding author. Tel.: + 33-383-912097; fax: + 33-383-912093.

E-mail address: guy.branlant@maem.uhp-nancy.fr (G. Branlant).

ing the factors responsible for the stabilization and chemical activation of the covalent intermediates, using X-ray crystallography, site-directed mutagenesis, kinetic and physico-chemical approaches. The results support the involvement of an oxyanion site including the side-chain of Asn-169. Finally, given the strict substrate-specificity of GAPN compared to other ALDHs with wide substrate specificity, one has also initiated the characterization of the G3P binding properties of GAPN. These results will be presented and discussed from the point of view of the evolution of the catalytic mechanisms of ALDH. © 2001 Elsevier Science Ireland Ltd. All rights reserved.

**Keywords:** Aldehyde dehydrogenase; Chemical mechanism; Oxyanion; Nucleophiles; Substrate binding

---

## 1. Introduction

Non-phosphorylating glyceraldehyde 3-phosphate dehydrogenase (GAPN) from *Streptococcus mutans*, an NADP-dependent aldehyde dehydrogenase (ALDH), is postulated to supply the lack of NADP reducing enzymes of the oxidative hexose phosphate pathway in this organism [1]. It catalyzes the irreversible oxidation of glyceraldehyde-3 phosphate (G3P) into 3-phosphoglycerate (3-PGA) in the presence of cofactor NAD(P) via a two-step chemical mechanism. First, the acylation step involves the formation of a covalent thiohemiacetal intermediate which precedes the oxidoreduction process that leads to a thioacyl intermediate and NAD(P)H. Secondly, the deacylation step includes the attack of a water molecule on the thioacyl intermediate, release of the acid product and of the reduced cofactor and any potential isomerization step. GAPN is a tetrameric enzyme close to the class 2 mitochondrial ALDH, whose kinetic mechanism is generally rate-limited by the hydrolysis.

The fact that many class 2 ALDHs show high catalytic efficiency, implies prerequisites with respect to the chemical catalysis. First, the essential Cys should be both accessible and in the thiolate form to efficiently attack the aldehyde group at a physiological pH. Given the  $pK_a$  of a free thiolate residue, i.e. 8.9, this implies that the protein environment of the catalytic site is designed so that the essential Cys is accessible and that its  $pK_a$  is decreased, such that it is reactive at a neutral pH. Secondly, the hydride transfer from the hemithioacetal intermediate towards the C-4 position of the nicotinamide ring of the cofactor should also be activated. Thirdly, the nucleophilic character of the water molecule involved in the deacylation step must be strongly enhanced. This also raises the question of whether other nucleophilic compounds could be accepted as deacylating compounds. Additionally, the different intermediates should be stabilized. Finally, unlike other ALDHs with wide substrate specificity, GAPN is very specific for its substrate G3P, (although D-G3P is the natural substrate, GAPN does not show specificity with respect to the D,L stereoisomers) which brings up the problem of the evolution of the substrate recognition site in these enzymes.

## 2. The acylation

### 2.1. Evidence for the chemical activation of Cys-302 upon cofactor binding

Oxidation of D-G3P into 3-PGA by GAPN involves the formation of a covalent enzyme intermediate via Cys-302. Although activity is optimum at pH 8.2, it is about half at pH 7.2. Surprisingly, titration of Cys-302 residues by kinetic probes, such as iodoacetamide, showed a unique  $pK_a$  of 8.5 in the apo-enzyme, with a chemical reactivity much lower compared to a reactive and an accessible thiolate. However, binding of NADP caused a strong increase in the reactivity of Cys-302 and a pH-reactivity profile with two  $pK_a$  of 6.1 and 7.6. Since only the thiolate form of Cys-302 is reactive towards iodoacetamide, the alkylation method allows direct determination of Cys-302  $pK_a$ . In addition, no reactivity was observed at pH lower than 5.5, indicating that no thiolate species exists at these pH. Thus, this experiment showed the titration of Cys-302 with a  $pK_a$  value shifted from 8.5 to 6.1, and of a residue with  $pK_a$  7.6, whose deprotonation resulted in a 3-fold increase of the rate of alkylation [2]. Therefore, cofactor binding is able to induce, at least, a reorientation of the side chain of Cys-302 which results in a decreased  $pK_a$ , renders Cys-302 more accessible at a neutral pH, and reveals the presence of a residue of  $pK_a$  7.6.

Another mean to follow the conformational rearrangement is to measure the quenching of the tryptophan fluorescence intensity upon coenzyme binding. GAPN contains three tryptophan residues located either in the coenzyme-binding domain (Trp-28, Trp-76), or in the catalytic domain (Trp-397) [3]. When wild-type apo-enzyme was excited at 297 nm, a fluorescence emission maximum was observed at 330 nm. Incubating apo-wild type with NADP at saturating concentration under experimental conditions where the conformational rearrangement has occurred led to a fluorescence quenching. This quenching is in fact the consequence of two additive effects: first, of the instantaneous binding of NADP to the apo-structure which leads to 75% of the quenching, second, of a conformational rearrangement, which is a function of time and which represents 25% of the quenching. A rate constant of  $1.7 \text{ h}^{-1}$  was determined for the conformational rearrangement step at pH 5.5 and at  $4^\circ\text{C}$ , which is similar to that determined from Cys-302 reaction kinetics. This indicated that, concomitant with the increase in the Cys-302 reactivity, the environment of the quenched Trp changed. Analysis of the fluorescence properties of W28F, W76F and W397F mutant GAPN revealed that only Trp-397 was responsible for the additional quenching associated with the rearrangement. This could be due to a repositioning of either the cofactor or the quenched Trp or both. From the comparison of crystallographic structures of C302S GAPN–NADP–G3P and of wild-type GAPN–NADP complexes in which the transition has occurred or not, respectively, it can be concluded that the position of Trp-397 is not affected by the conformation change while the movement of the nicotinamide mononucleotide moiety of NADP is an essential event in this rearrangement of the active site [4] (Fig. 1A).

The fact that no lag phase was observed in the turnover kinetics between pH 5 and 9 on the time-scale of a stopped-flow apparatus indicated that the binding of

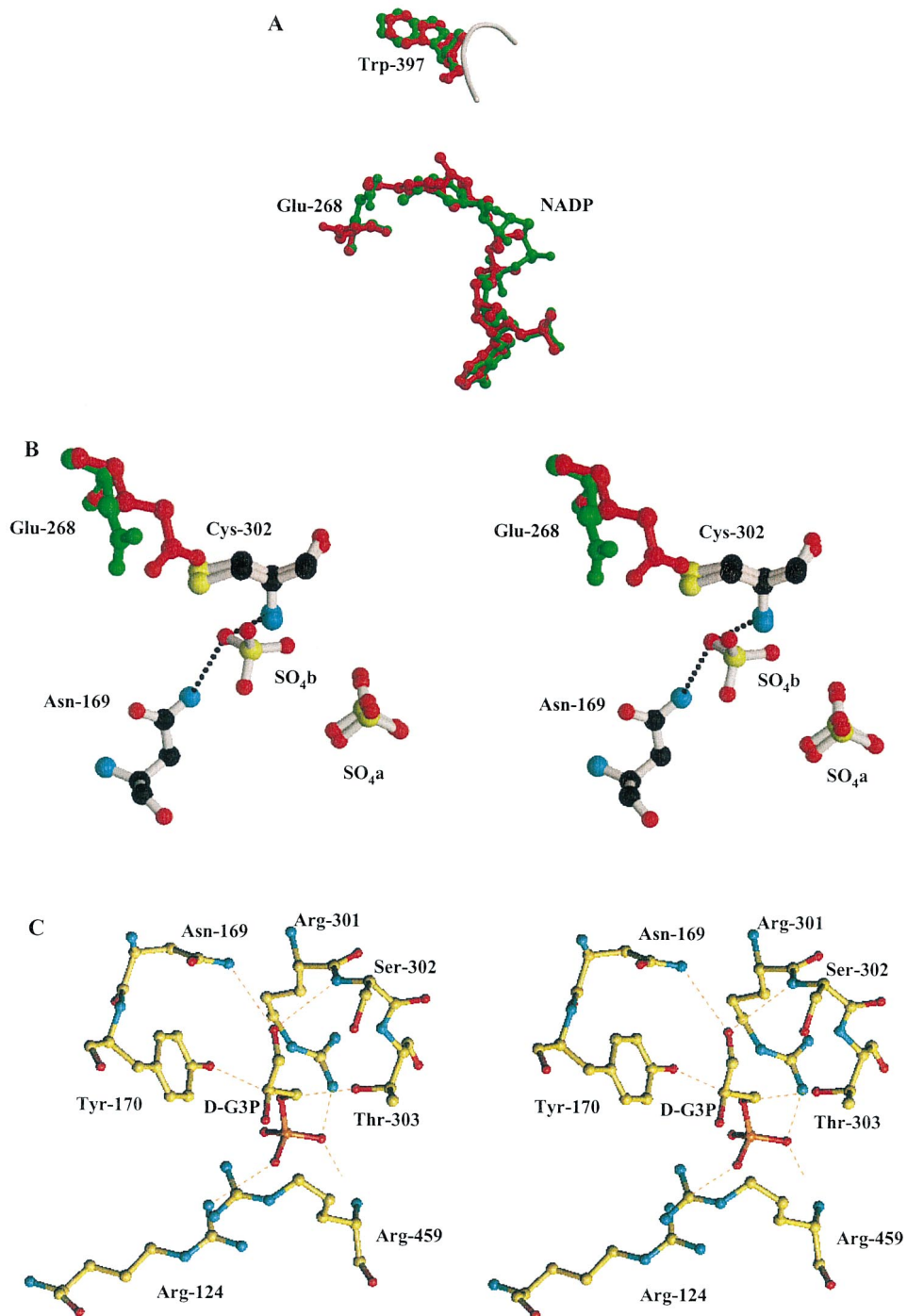


Fig. 1. (Continued)

G3P to the binary complex enzyme-NADP, even under an apo-like conformation, led to the formation of an efficient ternary complex that considerably increased the rate of the conformational rearrangement. This was further supported by the behaviour of the inactive C302A mutant which also exhibited a fluorescence quenching upon NADP binding at saturating concentration but which remained constant over time and represented 75% of the total fluorescence quenching observed for the holo-wild type. When a large excess of G3P was added to the C302A mutant saturated by NADP, an instantaneous additional quenching of similar amplitude relative to the holo-form of the wild type was observed [2].

## 2.2. The role of Glu-268 in acylation

Investigation of the chemical mechanism of aldehyde dehydrogenases relies on the possibility of resolving the main steps of the reaction, the acylation and the deacylation. In that regard, the GAPN enzyme appears as a fine mechanistic model: it was shown that for both the wild-type and the mutant enzymes studied, conditions can be found such that acylation and deacylation are kinetically resolved, and that under all steady state conditions, the deacylation is the rate-limiting step for the whole reaction. This allowed one to study the effect of pH and of active site residue Glu-268 substitution on both phases of the reaction.

Study of the rate of acylation  $k_{ac}$  as a function of pH is used to reveal ionizations which control the rate-limiting step for the decomposition of the ternary complex enzyme-NADP-G3P, which could include nucleophilic attack of essential Cys on the substrate, hydride transfer or any associated conformational step. Two wild-type enzyme species acylated efficiently from pH 5 to 9, with two apparent  $pK_a$ s of 6.2 and 7.5. Substitution of Glu-268 by Ala resulted in simplification of the pH- $k_{ac}$  curve to a monosigmoidal profile characterized by a  $pK_a$  of 6.2. This suggests the assignment of the  $pK_a$  7.6 to the Glu-268 side-chain both in the  $k_{ac}$  and, owing to their similarity, in the alkylation profiles discussed above [5].

Most importantly, the high efficiency of acylation of E268A mutant GAPN, which is not rate-limiting over the full pH range demonstrates that in GAPN, Glu-268 is not critically involved in the catalysis of the acylation step. In fact, deprotonation of the Glu-268 side chain yielded a new protonic species with an acylation rate increased by only 4-fold, compared to the already efficient intermediate species (210 vs. 52 s<sup>-1</sup>).

---

Fig. 1. (A) Superimposition of NADP and residues 268 and 397 of Wild type GAPN-NADP complex (red) and of the inactive C302S-NADP-G3P ternary complex (green). The Trp-397 residue is used as fluorescent probe to follow the reorganisation of the GAPN active site. (B) A stereoview showing the superimposition of the active site structures of Apo1 and Apo2. One sulphate ion of Apo2 interacts with the amide side chain of Asn-169 and the NH group of Cys-302. (C) A stereoview of the substrate binding site of the inactive C302S-NADP-G3P ternary complex of GAPN. The carbonyl group of D-G3P is in interaction with the Asn-169 amide side chain and the NH main chain of Ser-302. The phosphate moiety is stabilized by hydrogen bonds with the side chain of Arg-124 and Arg-301 residues, the hydroxyl group of Tyr-170 and Thr-303 residues and the main chain NH of Arg-459 residue.

### 2.3. Structural characterization of the conformational rearrangement from crystallographic studies

The crystal structures of various forms of GAPN have been solved: two apoenzyme forms, Apo1 with one sulphate ion and Apo2 with two sulphate ions bound into the catalytic site, mimicking the phosphate or both the phosphate and the C1 groups of G3P, respectively; the binary complex GAPN–NADP named Holo; and the C302S mutant as a binary complex with NADP and as the ternary complex composed of the C302S enzyme, NADP and G3P [3,4].

Comparison of the Apo1 and Apo2 structures shows that in the catalytic site of Apo2, the major difference concerns the Glu-268, whose side-chain orientation is modified. Its carboxylate group is now positioned 3.7 Å from the Cys-302 sulphur atom (Fig. 1B) instead of 7 Å, in an environment comprising several hydrophobic groups. Consequently, the  $pK_a$  of 7.6 previously uncovered in the alkylation and acylation profiles most likely corresponds to the Glu-268 side-chain brought into interacting distance of Cys-302, this  $pK_a$  value being consistent with its new hydrophobic environment. The effect of the conformational rearrangement is also exemplified by the different NADP and Glu-268 conformations observed in the C302S–NADP–G3P complex compared to the Holo and C302S–NADP complexes (Fig. 1A). This supports the previous result that the formation of the ternary complex favours the conformational rearrangement toward a catalytically competent form.

However, since the acylation step is not affected when Glu-268 is mutated into Ala or Gln [5], the cysteine activation thus requires another pathway. In the Holo structure, the Cys-302 side chain rotates toward the catalytic site, during the cofactor binding, thus positioning it near the Cys-302 and Thr-303 NH groups [4]. This movement is likely responsible for its increased accessibility in comparison with Apo1, and for its  $pK_a$  decrease at least in the ternary complex. Although the resolution of both the Holo and ternary complex structure do not allow hydrogen bonds between Cys-302 and either NH-302 or NH-303 main chain to be actually observed, the crystallographic and biochemical studies strongly favour this hypothesis concerning the  $pK_a$  decrease. In addition, it has been noted that the positively charged nicotinamide ring also influences the Cys-302  $pK_a$  as it is 6.8 in the presence of NADPH instead of 6.1 when NADP is added [2].

### 2.4. The oxyanion hole

Over a pH range from 5 to 9.5, substitution of Asn-169 by Thr or Ala resulted in a decrease of the  $k_{cat}$  value by two or three orders of magnitude, respectively [4]. No changes in the apparent  $K_M$  values for substrate and cofactor were observed. These mutations also suppressed the presteady state burst of NADPH production observed for the wild-type enzyme, indicating that the rate-limiting step is shifted from the deacylation step in the wild type to the acylation step in the mutant enzyme. The acylation was at least  $10^3$ – $10^4$ -fold slower compared to the wild type. The fact that an isotope effect was observed for the N169A or N169T mutants

when D-[1-<sup>2</sup>H]G3P is used as the substrate proves that the mutations result in change of the nature of the rate-determining transition state, which is shifted to the hydride transfer. An isotope effect is also observed for the wild type in the acylation step [4].

The combined observations of a substrate isotope effect on the acylation for both the wild type and the mutant enzymes, of the very low rate of acylation for the mutant enzymes and of similar  $K_M$  values for the wild-type and the mutant enzymes, show that the mutations only affect the energy level of the hydride transfer, and thus reveal a direct interaction between the Asn-169 amide group and the oxygen atom of the thiohemiacetal intermediate. This hypothesis is strongly supported by inspection of the Apo2 and the ternary complex C302S/NADP/G3P structures which show the NH<sub>2</sub> group of the Asn-169 side chain pointing towards one of the SO<sub>4</sub><sup>2-</sup> oxygen atoms (which could mimic the C1 oxygen atom of the hemithioacetal intermediate) (Fig. 1B) and the oxygen atom of the G3P aldehyde group (Fig. 1C), respectively. In addition, in the C302S ternary complex, the aldehyde carbonyl oxygen of the substrate interacts with Ser-302 NH group (Fig. 1C) and therefore likely with the Cys-302 NH group of the wild-type enzyme as the rms value between their positions is small (0.27 Å) [4]. Altogether, these results give evidence of an *oxyanion hole* composed of at least residue Asn-169, as previously proposed on the basis of modeling [6]. Within the acylation, Asn-169 would first stabilize the tetrahedral intermediate and secondly, decrease the p*K*<sub>a</sub> of the thiohemiacetal hydroxyl group such that it is deprotonated at physiological pH, thus permitting an efficient hydride transfer towards the C4 position of the oxidized cofactor without base catalyst assistance.

### 3. The deacylation

#### 3.1. Hydrolysis

To begin with, the drastic decrease of the steady state rate constant  $k_{ss}$  over the pH-range tested for the reaction catalyzed by the E268A mutant demonstrated the *essential role of Glu-268 in the deacylation step*. To get further insight into the catalytic role of Glu-268, the solvent isotope effect (SIE) of D<sub>2</sub>O on  $k_{ss}$  as a function of pH for the wild-type enzyme was analyzed. The SIE of  $2.3 \pm 0.1$  at basic pH and the pH–SIE profile characterized by a unique p*K*<sub>a</sub> of  $7.7 \pm 0.1$  confirm that the rate-limiting step is associated with deacylation. Moreover, the similarity between this p*K*<sub>a</sub> and the p*K*<sub>a</sub> value of 7.6 obtained in the acylation profile strongly suggests the assignment of this ionization to the same residue, namely Glu-268. The SIE of  $2.3 \pm 0.1$  observed at basic pH would indicate that the glutamate form of Glu-268 acts as a base catalyst at high pH. Use of the proton inventory method for wild-type GAPN at pH 8.5 showed that the dependence of  $k_{ss}$  upon the D<sub>2</sub>O mole fraction is essentially linear, supporting that the SIE originates from the transfer of one proton in the rate-limiting transition state. Therefore, at a basic pH, deacylation would be catalyzed by the chemical activation of the water



molecule attacking the thioacyl intermediate, via abstraction of one proton by Glu-268 [5]. This process would thus be associated with the rate-limiting step within deacylation. For the GAPN-catalyzed reaction, the proton inventory result suggests that catalysis by a coupled multiproton transfer mechanism, which would involve another residue from the active site, is not likely.

Another essential, although surprising, observation was the relatively high activity of wild-type GAPN in the acidic side of the pH-range tested. Indeed, the pH-dependence profile of  $k_{ss}$  is characterized by two  $pK_a$  values of 6.1 and 7.4, indicating the existence of an active ‘intermediate’ species with characteristic rate constant of  $23\text{ s}^{-1}$ , aside from the basic species characterized by  $68\text{ s}^{-1}$ . At pH 6.5, where GAPN likely exists primarily as the intermediate species with Glu-268 under the acidic form, the deuterium solvent isotope effect of 1.1 indicates that the rate-limiting process is no longer associated with proton transfer. Therefore, it was proposed that at this pH, Glu-268 catalyzes deacylation through activation and orientation of the attacking water molecule in the active site [5].

### 3.2. Deacylation by other nucleophilic compounds

Both E268A [5] and E268Q mutant GAPN showed poor activation of the attacking water molecule in the deacylation. Therefore, the question arises of whether other compounds could replace water in the active site of these enzymes. Among the series of small nucleophilic compounds tested, hydroxylamine and hydrazine did not behave as substrates for wild-type GAPN. For the E268A and E268Q mutant GAPN, however, the kinetic characterization of the reaction under steady state conditions in the presence of these nucleophiles, summarized in Table 1, revealed that both compounds behaved like substrates in the GAPN-catalyzed reaction, potentially in place of the water molecule in the deacylation. The various evidence in support of this result is listed as follows.

First, the mutant enzymes showed saturation kinetics with respect to the nucleophilic compounds (Table 1). Second, presteady state analysis showed that the acylation was not affected by the presence of the nucleophiles. Third, the putative product of the hydroxylaminolysis, 3-phosphoglycerohydroxamate, was titrated colorimetrically at 525 nm by complexation of  $\text{FeCl}_3$  with the hydroxamate group. The experiment actually proved the apparition of the hydroxamate, with a stoichiometry of 1 mol for 1 mol of G3P. These conclusions were also supported by detection of these products by thin layer chromatography. Finally, the recent determination of the crystal structure of the E268A GAPN-NADP-NH<sub>2</sub>OH complex showed that hydroxylamine could bind in the active site of this mutant enzyme (data not shown).

It was established next that the rate-limiting step of the GAPN-catalyzed reaction in the presence of hydroxylamine or hydrazine remained deacylation, probably the nucleophilic attack on the thioacyl intermediate. Thus, activation of the steady state rate constants for hydroxylaminolysis and hydrazinolysis compared to hydrolysis could only result from the intrinsic reactivity of these compounds, potentially activated within the active site, or from their stabilization in this site. Comparison

Table 1  
Kinetic parameters for E268A and E268Q mutant GAPN in the presence of exogenous nucleophiles<sup>a</sup>

	H <sub>2</sub> O			Hydroxylamine			Hydrazine		
	$k_{ss}$ (s <sup>-1</sup> )	$k_2$ (M <sup>-1</sup> s <sup>-1</sup> )	$K_M$ (mM)	$k_{ss}$ (s <sup>-1</sup> )	$k_2$ (M <sup>-1</sup> s <sup>-1</sup> )	$K_M$ (mM)	$k_{ss}$ (s <sup>-1</sup> )	$k_2$ (M <sup>-1</sup> s <sup>-1</sup> )	$K_M$ (mM)
Wild-type GAPN	68	1.21	I.E <sup>b</sup>	/	/	I.E <sup>b</sup>	/	/	/
E268A mutant	0.08	$1.43 \times 10^{-3}$	30	4.0	137	112	2.8	10	10
E268Q mutant	0.73	$13 \times 10^{-3}$	39	5.4	115	120	1.2	9	9
Alkyl-thiolacetate		$>10^{-8}$			$1.3 \times 10^{-3c}$			$2 \times 10^{-3d}$	

<sup>a</sup> Kinetic parameters were deduced from nonlinear regression analysis according to the Michaelis–Menten equation taking into account a competitive inhibitor effect of the nucleophiles. The steady-state rate constant  $k_{ss}$  were measured at 25°C and pH 9.0 in a mixed buffer (120 mM Tris/HCl, 30 mM imidazole, 30 mM acetic acid) at a ionic strength of 0.15 M. The second-order rate constants  $k_2$  were determined at subsaturating concentrations of nucleophiles in the same experimental conditions as above.

<sup>b</sup> I.E., inhibitory effect.

<sup>c</sup> Data from [8].

<sup>d</sup> Data from [7].

of the second order rate constants  $k_2$  of chemical models of alkylthioesters and of the enzymatic model of GAPN shows that hydroxylaminolysis and hydrazinolysis are activated by 4–5 orders of magnitude compared to hydrolysis on chemical models [7,8], and by 3–5 orders of magnitude for the enzymatic model. Therefore, the observed rate constants likely reflect their intrinsic nucleophilic character rather than a specific chemical activation by the enzyme. This conclusion is further supported by the observation that the  $pK_a$  of the protonic species (6.1 and 8.3, respectively), which control the rate of the reaction, appear likely unchanged compared to the  $pK_a$  of the free compounds, hydrazine and hydroxylamine [7,8].

Nevertheless, the activation of the second order rate constants  $k_2$  for GAPN compared to the chemical models (Table 1) ( $10^5$  for hydroxylamine and  $\sim 5 \times 10^3$  for hydrazine) attested to a significant entropic role of the enzyme in the stabilization of the attacking nucleophile, thus increasing its local concentration in the environment of the thioacyl intermediate.

#### 4. The G3P substrate binding site

On the basis of the sequence alignment of GAPN from various origins, and of the crystal structures GAPN [4,5], three Arg residues were predicted to play key roles in the binding of G3P. In this work, Arg-124, Arg-301 and Arg-459 were substituted by Leu, Leu and Ile, respectively. All three mutations lead to drastic effects on the enzyme catalytic efficiency, although via distinct effects on the enzyme mechanism (Table 2).

For the R124L mutant GAPN, presteady state analysis showed that deacylation remained the rate-limiting step, thus allowing the independent analysis of the role of Arg-124 on both the acylation and the deacylation. The substitution of Arg-124 by Leu resulted in drastic consequences on the  $K_M$  for G3P, which could only be estimated to  $> 15$  mM for the deacylation, and to ca. 8 mM for the acylation at optimum pH (Table 2). Thus, experimental G3P concentrations were necessarily set to subsaturating concentrations, allowing only second order rate constants to be compared. The mutation leads to little consequences on the second order acylation rate constant  $k_2$  (which reflects the  $k_{ac}/K_M$  ratio), which retained the same order of magnitude, on the  $k_{ac}$ -pH profile, and on the [ $^2H$ -C1] G3P substrate isotope effect. Thus, Arg-124 plays no essential role in the rate-determining transition state, which remains associated to the hydride transfer. Therefore, Arg-124 would not be involved in the stabilization of the transition state associated to the hydride transfer, but only in stabilizing G3P binding in the active site. This interpretation is fully consistent with the structure of the C302S–NADP–G3P ternary complex, showing the Arg-124 guanidinium group involved in a hydrogen bond with one phosphate oxygen of G3P (Fig. 1C).

The picture is very different for the R301L and R459I mutant GAPN. The apparent  $K_M$  for G3P were also strongly affected, increased to  $> 15$  and ca. 9 mM, respectively, with observed rate constants of 0.02 and 0.05  $s^{-1}$  at subsaturating concentration of 4 mM G3P. However, the rate-limiting process was associated

Table 2  
Summary of the rate constants and kinetic parameters for the wild-type, R124L, R301L and R459I GAPN-catalyzed reactions

	Rate-limiting step	Acylation		Deacylation			
		$K_M$ (mM pH 8.5)	$k_{ac}$ (s <sup>-1</sup> )	$k_2$ (M <sup>-1</sup> s <sup>-1</sup> )	Substrate isotope effect	$K_M$ (mM pH 8.5)	$k_{ss}$ (s <sup>-1</sup> )
Wild-type GAPN	Deacylation	0.49 <sup>a</sup>	210 <sup>a</sup>	1 × 10 <sup>6</sup>	2.7 <sup>a</sup>	0.046	60 ± 0.1
R124L mutant	Deacylation	~8	410 <sup>b</sup>	2 × 10 <sup>5</sup>	2.1	> 15 <sup>c</sup>	2.8 <sup>c</sup>
R301L mutant	Acylation	> 15 <sup>c</sup>	0.06 ± 0.007 <sup>c</sup>	15	1.2	/	/
R459I mutant	Acylation	~9	0.05 ± 0.01	12	1.3	/	/

<sup>a</sup> The acylation rate constant and  $K_M$  determination were performed under presteady-state conditions at 10°C, at 0.2 mM G3P due to the strong substrate inhibition. Other experimental details were described in [4].

<sup>b</sup>  $k_{ac}$  determined in the presence of subsaturating concentration of 2 mM D-G3P at 25°C.

<sup>c</sup> Rate constants were proportional to the substrate concentration up to 4 mM D-G3P.  $k_{obs}$  values were determined in the presence of subsaturating concentration of 4 mM D-G3P.

with the acylation. The lack of substrate kinetic isotope effect with [ $^2\text{H-C1}$ ]-G3P showed that within acylation, the hydride transfer step was no longer rate-limiting, but might be associated with the nucleophilic attack of Cys-302 thiolate on G3P C1 atom. The drastic decrease of the second order rate constants also revealed that mutations of Arg-301 and Arg-459 to Leu and Ile, respectively, both resulted in changes in the nature and in the energy level of the rate-determining transition state. Hence, both residues would not only participate in the stabilization of G3P binding, but also in positioning and orientating G3P with respect to Cys-302. Indeed, from the crystallographic analysis of GAPN C302S–NADP–G3P ternary complex and GAPN Apo2 structures, both residues might be involved in G3P binding by two anchoring points: on the one hand, Arg-459 main chain NH and Arg-301 guanidinium to one of the C3 phosphate oxygens, on the other hand Arg-459 guanidinium group and Arg-301 main chain (via Cys-302) to the C1–C2 moiety of the G3P molecule (Fig. 1C).

## 5. Conclusion

The chemical mechanism proposed for GAPN first depends on an activation step of the essential Cys-302 resulting from a conformational rearrangement of the active site into a catalytically competent enzyme form. This rearrangement would include at least reorientation of both lateral chains of Cys-302 and Glu-268 and repositioning of the nicotinamide ring of NADP. This local reorganization renders Cys-302 more accessible, leads to  $\text{p}K_{\text{a}}$  shifts of Cys-302 and Glu-268 from 8.5 to 6.2 and from a lower value depending on its environment in the apo form to 7.5, respectively, and brings the side chains of Cys-302 and Glu-268 to an interacting distance less than 4 Å. In this holo-complex, amide peptide nitrogens of residues 302 and 303, the positive charge of the nicotinamide ring of NADP and possibly other structural elements would stabilize the thiolate form of Cys-302. Next, within the acylation step in which the hydride transfer is the rate-limiting step, Asn-169 would participate in the stabilization of the tetrahedral intermediate and decrease the  $\text{p}K_{\text{a}}$  of the thiohemiacetal hydroxyl group such that it is deprotonated at physiological pH, thus permitting an efficient hydride transfer towards the C4 position of the oxidized cofactor without base catalyst assistance. Finally, in the deacylation step in which the hydrolysis process is rate-determining for the whole reaction, Glu-268 is involved in activation and orientation of the attacking water molecule in the active site. For each of these individual steps, the question arises of whether the scenario of the GAPN-catalyzed reaction is common to other non-phosphorylating ALDHs.

Regarding the involvement of structural elements in the activation of Cys-302, no biochemical evidence is yet available for other ALDHs, but the role of the positively charged nicotinamide ring of the cofactor in the close environment of Cys-302 was pointed out from crystallographic studies of class-9 ALDH [9]. In addition, the requirement for an orientation change of the Glu-268 and cofactor was suggested from the observation of the structures of class-1 ALDH [10].

The studies on Asn-169 mutants of GAPN have shown the involvement of this residue in an oxyanion site, as already suggested from transition state modeling studies [6]. Given the strong conservation of this residue among ALDHs, it is highly probable that the role of this residue is the same in the enzymatic mechanism of other ALDHs.

The role of Glu-268 might be more variable. Indeed, the relative importance of this residue on acylation compared to deacylation appears to differ between ALDHs. On human liver class-2 ALDH, its mutation to Asp/Gln leads to a switch of the rate-limiting step from deacylation to acylation [11], while it would only be involved in cofactor binding in dimeric class-3 ALDH [12]. In this case, however, since hydride transfer is rate-limiting for the whole reaction, it is not possible to verify if Glu-268 is also involved in deacylation.

Altogether, these studies show that in spite of the high conservation of active site residues among ALDHs, the chemical mechanism could have evolved differently with respect to the relative importance of the structural elements of the active site on the chemical steps of the mechanism.

### Acknowledgements

This research was supported by the Centre National de la Recherche Scientifique and the University Henri Poincaré Nancy I.

### References

- [1] V.L. Crow, C.L. Wittenberger, Separation and properties of NAD<sup>+</sup>- and NADP<sup>+</sup>-dependent glyceraldehyde-3-phosphate dehydrogenases from *Streptococcus mutans*, *J. Biol. Chem.* 254 (1979) 1134–1142.
- [2] S. Marchal, G. Branlant, Evidence for the chemical activation of essential Cys-302 upon cofactor binding to nonphosphorylating glyceraldehyde 3-phosphate dehydrogenase from *Streptococcus mutans*, *Biochemistry* 38 (1999) 12950–12958.
- [3] D. Cobessi, F. Tete Favier, S. Marchal, S. Azza, G. Branlant, A. Aubry, Apo and holo crystal structures of a NADP-dependent aldehyde dehydrogenase from *Streptococcus mutans*, *J. Mol. Biol.* 290 (1999) 161–173.
- [4] D. Cobessi, F. Tete Favier, S. Marchal, G. Branlant, A. Aubry, Structural and biochemical investigations of the catalytic mechanism of an NADP-dependent aldehyde dehydrogenase from *Streptococcus mutans*, *J. Mol. Biol.* 300 (2000) 141–152.
- [5] S. Marchal, S. Rahuel-Clermont, G. Branlant, The role of Glu268 in the catalytic mechanism of non-phosphorylating glyceraldehyde dehydrogenase from *Streptococcus mutans*, *Biochemistry* 39 (2000) 3327–3335.
- [6] C.G. Steinmetz, P. Xie, H. Weiner, D.T. Hurley, Structure of mitochondrial aldehyde dehydrogenase: the genetic component of ethanol aversion, *Structure* 5 (1997) 701–711.
- [7] L.R. Fedor, T.C. Bruice, Nucleophilic displacement reactions at the thiolester bond. II. Hydrazinolysis and morpholinolysis in aqueous solutions, *J. Am. Chem. Soc.* 86 (1964) 4117–4123.
- [8] T.C. Bruice, L.R. Fedor, Nucleophilic displacement reactions at the thiolester bond. III. Kinetic demonstration of metastable intermediates in the hydroxylaminolysis and methoxylaminolysis of thiolester and thiolactones in aqueous solutions, *J. Am. Chem. Soc.* 86 (1964) 4886–4897.

- [9] K. Johansson, M. El-Ahmad, S. Ramaswamy, L. Hjelmqvist, H. Jörnvall, H. Eklund, Structure of betaine aldehyde dehydrogenase at 2.1 Å resolution, *Protein Sci.* 7 (1998) 2106–2117.
- [10] S.A. Moore, H.M. Baker, T.J. Blythe, K.E. Kitson, T.M. Kitson, E.N. Baker, Sheep liver cytosolic aldehyde dehydrogenase: the structure reveals the basis for the retinal specificity of class 1 aldehyde dehydrogenases, *Structure* 6 (1998) 1541–1551.
- [11] X. Wang, H. Weiner, Involvement of glutamate 268 in the active site of human liver mitochondrial (class 2) aldehyde dehydrogenase as probed by site-directed mutagenesis, *Biochemistry* 34 (1995) 237–243.
- [12] C.J. Mann, H. Weiner, Differences in the roles of conserved glutamic acid residues in the active site of human class 3 and class 2 aldehyde dehydrogenase, *Protein Sci.* 8 (1999) 1922–1929.